

## Application of High Amplitude Alternating Magnetic Fields for Heat Induction of Nanoparticles Localized in Cancer

Robert Ivkov,<sup>1</sup> Sally J. DeNardo,<sup>2</sup> Wolfgang Daum,<sup>1</sup> Allan R. Foreman,<sup>1</sup> Robert C. Goldstein,<sup>3</sup> Valentin S. Nemkov,<sup>3</sup> and Gerald L. DeNardo<sup>2</sup>

**Abstract Objective:** Magnetic nanoparticles conjugated to a monoclonal antibody can be i.v. injected to target cancer tissue and will rapidly heat when activated by an external alternating magnetic field (AMF). The result is necrosis of the microenvironment provided the concentration of particles and AMF amplitude are sufficient. High-amplitude AMF causes nonspecific heating in tissues through induced eddy currents, which must be minimized. In this study, application of high-amplitude, confined, pulsed AMF to a mouse model is explored with the goal to provide data for a concomitant efficacy study of heating i.v. injected magnetic nanoparticles.

**Methods:** Thirty-seven female BALB/c athymic nude mice (5-8 weeks) were exposed to an AMF with frequency of 153 kHz, and amplitude (400-1,300 Oe), duration (1-20 minutes), duty (15-100%), and pulse ON time (2-1,200 seconds). Mice were placed in a water-cooled four-turn helical induction coil. Two additional mice, used as controls, were placed in the coil but received no AMF exposure. Tissue and core temperatures as the response were measured *in situ* and recorded at 1-second intervals.

**Results:** No adverse effects were observed for AMF amplitudes of  $\leq 700$  Oe, even at continuous power application (100% duty) for up to 20 minutes. Mice exposed to AMF amplitudes in excess of 950 Oe experienced morbidity and injury when the duty exceeded 50%.

**Conclusion:** High-amplitude AMF (up to 1,300 Oe) was well tolerated provided the duty was adjusted to dissipate heat. Results presented suggest that further tissue temperature regulation can be achieved with suitable variations of pulse width for a given amplitude and duty combination. These results suggest that it is possible to apply high-amplitude AMF ( $>500$  Oe) with pulsing for a time sufficient to treat cancer tissue in which magnetic nanoparticles have been embedded.

When living tissues are heated to temperatures between 42°C and 46°C the result is cellular inactivation in a dose-dependent manner (1, 2). Some success has been achieved in the development of cancer treatments based on this classic hyperthermia response (3-6). Tissues heated to above 46°C undergo extensive necrosis known as thermoablation. The promise of thermoablation has been realized for some local and regional diseases (7, 8).

The concept of thermoablative cancer therapy requires that a controlled amount of heat be focused in the tumor area without excessively heating the intervening tissues. A variety of strategies have been developed that use the alternating magnetic field (AMF) component of electromagnetic fields in the radiofrequency spectrum to localize and concentrate

ablative heat for cancer treatment by either directly heating the tissue or activating a susceptor material. These techniques take advantage of local heat production through either (a) induction heating of a material embedded within the tissue, or (b) direct tissue heating caused by the interaction of radio-frequency with the tissue, or (c) both.

Induction heating of magnetic (susceptor) materials embedded in cancer tissue, also called hysteresis heating, results from the interaction of the magnetic moment of the susceptor material with the AMF. On the other hand, interaction of AMF with tissue can produce heat directly, as with any electrically conductive material. The mechanism that dominates this type of heating results from the production of (electric) eddy currents producing heat that scales as

$$\text{SAR}_{\text{EC}} \propto f^2 \cdot H^2 \cdot r^2, \quad (\text{A})$$

where SAR is the tissue-specific absorption rate, measured as W/g tissue,  $r$  is the radius of exposed region, and  $f$  and  $H$  are the AMF frequency and amplitude, respectively. Thus, the energy source for the susceptor material is also the heat source for nonspecific heating of intervening tissue.

An approach using AMF to heat magnetic nanoparticles embedded in cancer tissue has the potential to provide selective heating to the microenvironments of cells containing the excited particles (9-11). The degree to which this approach is

**Authors' Affiliations:** <sup>1</sup>Triton BioSystems, Inc., Chelmsford, Massachusetts; <sup>2</sup>Radiodiagnosis and Therapy, Molecular Cancer Institute, University of California, Davis, Sacramento, California; and <sup>3</sup>Centre for Induction Technology, Inc., Auburn Hills, Michigan

**Grant support:** Triton BioSystems, Inc. Presented at the Tenth Conference on Cancer Therapy with Antibodies and Immunoconjugates, October 21-23, 2004, Princeton, New Jersey.

**Requests for reprints:** Robert Ivkov, Triton BioSystems, Inc., 200 Turnpike Road, Chelmsford, MA 01824. Phone: 978-856-4154; Fax: 978-250-4533; E-mail: rivkov@tritonbiosystems.com.

© 2005 American Association for Cancer Research.  
doi:10.1158/1078-0432.CCR-1004-0016

practical depends upon (a) the ability to systemically deliver nanoparticles to the cancer in sufficient concentrations to achieve thermoablation when AMF is applied and (b) a combination of magnetic nanoparticle and AMF characteristics that result in extremely rapid heating of the specific cancer microenvironment while maintaining temperatures tolerable to normal tissues.

AMF combinations that are ideal for rapid particle heating (i.e., high amplitude and long durations) can deposit power to tissues challenging mammalian thermoregulatory mechanisms. These mechanisms maintain the body temperature within a prescribed temperature range under conditions in which the thermal load on the body may vary. Exposure to high-amplitude AMF in the radiofrequency range provides a unique exception to energy flows normally encountered by mammals (12). Thus, it is beneficial to explore AMF variables that selectively induce eddy current heating without significantly reducing potential for particle heating.

This report describes the safety implications of a new technique to treat cancer that exploits the combination of magnetic nanoparticles localized in cancer using specific antibodies (bioprobes) and an AMF device that can be switched on and off to heat the targeted nanoparticles thereby inducing heat at the cancer sufficient to destroy the cancer cells. This novel treatment is unique, because the heat is focused on the cancer cells by virtue of the localization of the nanoparticles so that when the magnetic field is applied, the bioprobes heat and destroy the cancer cells but provide relative sparing of the healthy tissues. This study was intended to define the implications of the nonspecific heating incident to the AMF.

The limits of safe application of confined, pulsed, high-amplitude (400-1,300 Oe) alternating magnetic fields with frequency of 150 kHz *in vivo* in a mouse model were explored in anticipation of a future study intended to treat cancer using submilligram quantities of bioprobes embedded in cancer tissue. An AMF inductor was built to confine high-amplitude magnetic fields to a 1-cm wide band of the interior of a 35-mm internal diameter induction coil. Mice were subjected to varying combinations of AMF by adjusting amplitude, duty, pulse ON/OFF time combinations, and total duration of exposure.

High-amplitude AMF was well tolerated even at 1,300 Oe for up to 20-minute exposures provided the duty and ON/OFF combinations were adjusted to allow sufficient OFF time to dissipate heat. At lower field amplitudes of  $\leq 700$  Oe, no adverse effects were observed even at continuous power application (100% duty) for up to 20 minutes.

## Materials and Methods

### Mice

A total of 39 female BALB/c *nu/nu* mice (Harlan Sprague-Dawley, Frederick, MD), 5 to 8 weeks old and weighing 20.0 to 29.2 g (mean, 26.3 g), were maintained according to University of California guidelines on a normal diet, *ad libitum*.

Each mouse was anesthetized by injecting 0.02 mL i.p. per gram body weight of a solution prepared by dissolving 0.5 g of 2,2,2-tribromoethanol in 1.0 mL warm *tert*-amyl alcohol then diluting the solution with 40 mL distilled water and filtering through a 0.2- $\mu$ m filter. Anesthesia was determined by lack of reflexive response when a hind paw was lightly compressed.

After the mouse was anesthetized, four fiber optical temperature probes (FISO, Inc., Quebec, Canada) were placed. One was inserted s.c. proximal to the lower spine (spine) by inserting a 16-gauge  $\times$  1.5 in. hypodermic needle at the base of the tail and threading the fiber optical probe through the needle under the skin. This procedure was repeated for a second probe placed s.c. in the flank (flank). A third probe was taped onto the skin of a hind limb (skin) using wound dressing, and a fourth probe was inserted one cm into the rectum (rectal). After the probes were in place, the mouse was wrapped lightly in absorbent paper and inserted into a 50-mL centrifuge tube with the bottom removed. This tube with the mouse was inserted into the felt-lined AMF coil, so that the intended abdominal tumor location of each mouse was positioned in the 1-cm high-amplitude region of the induction coil. Once the mouse was in place and the variables programmed into the controls, the AMF generator was turned on. The magnetic field and time variables sampled in this study are summarized in Table 1.

After exposure, each mouse was left in the coil until the core (rectal) temperature began to decrease and all probes were removed. The mouse was removed from the coil and centrifuge tube and placed on a warm recovery pad on its back. When the righting reflex returned, the mouse was returned to its cage.

The mice were observed for 48 hours for signs of morbidity. Mice that died (total of five, cf. Table 1) during that period were necropsied. One mouse that showed no sign of injury was randomly selected and euthanized for comparison (Table 1).

Temperatures were recorded at 1-second intervals for each probe, beginning after each mouse was positioned in the coil and 30 seconds before AMF exposure. All mice placed in the coil exhibited decreasing temperature (hypothermia) before initiation of AMF exposure, likely due to the combination of anesthesia (12) and the 14°C inductor coil. Initial temperatures varied from 26°C to 32°C. Two mice that received no AMF exposure but were otherwise prepared in the same manner were placed in the coil to provide control data to compensate for this temperature change. For each mouse receiving AMF, the initial temperature was subtracted from temperature at time  $t = 1, 10, 20$  minutes and corrected using averaged control data. A summary of the corrected temperatures due to AMF,  $\Delta T_{\text{corr}}$ , is provided in Table 2.

### Alternating magnetic field system

A system was designed and built to provide high-amplitude AMF in an  $\sim 1$ -cm-wide band to the lower abdomen of a mouse. The lower abdomen was the intended site of future cancer xenograft, and by confining exposure to high-amplitude AMF to this region, exposure of tissue outside the intended area was minimized. The system consisted of three main components: (a) the induction coil, or inductor (Fig. 1A and B); (b) a capacitance network that, when combined with the inductor, forms a resonant circuit; and (c) the power supply.

**Inductor.** The inductor was designed using Flux 2D (Magsoft, Inc., Troy, NY) finite element analysis software. The induction coil was manufactured from square cross-sectional, oxygen-free, and high-conductivity copper tubing. The length of the induction coil was 40 mm with an internal diameter of 36 mm, which enabled insertion of a 50-mL conical centrifuge tube containing a mouse and allowing for 2.5 mm of thermal insulation around the circumference of the 50-mL tube.

A low-reluctance flux-concentrating ring made of Fluxtrol 50 (Centre for Induction Technology, Auburn Hills, MI) was added to the end of the solenoid coil where the mouse was inserted to divert magnetic flux away from areas not intended to receive high-amplitude AMF exposure. A low-reluctance magnetic return path was also added to one fourth of the outer diameter of the coil. These components provided a preferential path for the magnetic flux that minimized AMF exposure to much of the mouse body and directed the flux in the interior of the solenoid producing a 1-cm band of high-amplitude AMF in the ventral region, the intended tumor location.

**Table 1.** Summary of AMF conditions applied to mice with final uncorrected rectal temperature

No.	Field (Oe)	Duration (min)	ON time (s)	OFF time (s)	Duty (%)	Rectal temperature (°C)	Response code (arbitrary*)
1	0	20	0	0	0	26.6	0
2	0	10	0	0	0	28.4	0
3	400	10	600	0	100	30.4	0
4	400	20	30	30	50	26.9	0
5	400	20	5	25	15	26.8	0
6	400	20	20	10	67	25.1	0
7	400	20	40	20	67	24.8	0
8	700	20	1200	0	100	36.9	0
9	950	20	1200	0	100	45.4	2
10	950	20	30	15	67	37.4	0
11	950	20	15	15	50	34.9	0, 4
12	950	10	15	15	50	31.1	0
13	950	10	15	15	50	32.6	0
14	950	10	15	15	50	32.1	0
15	950	10	15	30	67	31.8	0
16	950	10	15	15	50	32.7	0
17	950	20	10	10	50	31.8	0
18	950	10	120	240	33	31.7	0
19	950	10	60	28.5	67	30.1	0
20	950	20	120	57.1	67	36.0	0
21	950	20	60	120	33	34.2	0
22	1,150	15	90	90	50	35.3	0
23	1,150	15	90	90	50	33.9	0
24	1,300	10	600	0	100	41.6	2
25	1,300	20	30	30	50	41.0	1
26	1,300	20	15	30	33	33.7	0
27	1,300	20	30	15	67	45.8	2
28	1,300	20	15	15	50	40.8	0
29	1,300	20	2	13	15	29.8	0
30	1,300	1	60	0	100	29.0	0
31	1,300	1	15	15	50	31.7	0
32	1,300	20	15	15	50	36.5	0
33	1,300	20	20	10	67	43.5	2
34	1,300	20	5	10	33	34.5	0
35	1,300	10	60	120	33	32.7	0
36	1,300	10	120	57.1	67	36.8	0
37	1,300	20	60	28.5	67	48.9	2
38	1,300	20	120	240	33	33.6	0

\* Coded physiologic response within 48 h of AMF exposure, arbitrary units: 0, no signs of injury or distress; 1, signs of injury, such as burns or hyperthermic stress; 2, death occurred within 48 h, animal necropsied; 4, animal euthanized for necropsy.

Measurements of the AMF flux with a current probe confirmed that if the rear third of the mouse was inserted into the induction coil, a 1-cm region of the abdomen could receive as much as 1,380 Oe, whereas tissue outside the concentrating ring (over 50% of the mouse) would not be exposed to >200 Oe. The field amplitude within the 1-cm band was measured before each set of trials and for each generator power setting used. It is the amplitude within this region that is reported as AMF amplitude.

During operation, the induction coil itself heats because it is a conductor carrying a high current load, particularly at high amplitude and high duty. To compensate, the inductor was cooled using a closed-loop circulating water system maintained at  $14 \pm 2^\circ\text{C}$  during operation.

**Capacitance network and power supply.** The capacitance network was built into the power supply and was adjusted for stable oscillation

at  $153 \pm 0.5$  kHz. The power supply was a 25-kW (0-25 kW) generator manufactured by PPECO (Watsonville, CA). A pulse-timer circuit manufactured by Giltron, Inc. (Medfield, MA) was installed allowing 0.5- to 9,999-second pulses at any duty (0-100%), defined as:

$$\text{Duty} = \frac{\text{Pulse ON time (seconds)}}{\text{Pulse ON time (seconds)} + \text{Pulse OFF time (seconds)}} \times 100\% \quad (\text{B})$$

### Experimental design and data analysis

**Statistical design and data analysis.** For both study design and data analysis, we used a statistical approach that did not require *a priori* knowledge of the effects and interactions of input variables and responses (i.e., AMF conditions and *in vivo* temperature, respectively). A total of five input variables were simultaneously varied: (a) field

amplitude (Oe), (b) total duration of exposure (minutes), (c) duty (%), (d) pulse ON time (seconds), and (e) pulse OFF time (seconds). The first three of these variables were sufficient to define the total AMF exposure. The latter two variables have an influence upon the unsteady state thermal evolution, particularly with respect to physiologic and environmental heat dissipation.

Trial design was done using Stat-Expert software (Stat-Ease, Inc., Minneapolis, MN) using both D-optimal and Box-Behnken designs to select trial conditions and numbers of mice that minimized both numbers of mice and morbidity.

Mice were divided into two groups, defined by short ON pulses (0-30 seconds) with field amplitudes of 400, 950, and 1,300 Oe and long ON pulses (60-240 seconds) with field amplitudes of 700, 1,150, and 1,300 combinations. In the second group of mice, factors selected from those used in the first group were repeated to maintain statistical continuity, allowing us to combine data from both groups for analysis. Also in the first group of mice, some mice were exposed to continuous power AMF (100% duty) for up to 1,200 seconds.

Temperature was measured as the response to AMF exposure. For analysis, a mathematical model of the form

$$Y = b_0 + b_1X_1 + b_2X_2 + b_3X_3 + b_{12}X_1X_2 + b_{13}X_1X_3 + b_{23}X_2X_3 + b_{11}X_1^2 + b_{22}X_2^2 + b_{33}X_3^2 + \dots \quad (C)$$

was fit to the temperature data using the method of least squares, where Y is the response, or temperature, and X<sub>1</sub>, X<sub>2</sub>, ... represent the factors duty, field amplitude, and duration. Temperature response to the combination of field amplitude, duration, and duty was analyzed. The effects of each term were determined using standard ANOVA techniques. Analysis and graphical representation of the data were done using Stat-Expert software (Stat-Ease). Physiologic responses were also noted; however, a systematic study of these was not undertaken.

Further analysis of the data including ON/OFF time combinations was undertaken to ensure the validity of the model, because all

**Table 2.** Summary of temperature change data for spine, flank, skin, and rectal temperature probes

No.	Field (G)	Duration (min)	ON time (s)	OFF time (s)	Duty (%)	$\Delta T_{\text{spine}}$ (°C)	$\Delta T_{\text{flank}}$ (°C)	$\Delta T_{\text{skin}}$ (°C)	$\Delta T_{\text{rectal}}$ (°C)
1	0	20	0	0	0	-5.6	-5.4	-5.8	-5.3
2	0	10	0	0	0	-3.0	-3.8	-3.5	-3.3
3	400	10	600	0	100	2.9	2.3	5.2	0.3
4	400	20	30	30	50	-4.1	-4.6	-3.7	-4.3
5	400	20	5	25	15	-6.2	-5.9	-6.3	-6.4
6	400	20	20	10	67	-4.6	-5.0	-4.1	-5.1
7	400	20	40	20	67	-6.2	-6.3	-5.8	-6.4
8	700	20	1,200	0	100	10.9	9.7	12.8	9.9
9	950	20	1,200	0	100	20.5	18.1	22.8	15.4
10	950	20	30	15	67	10.7	9.5	15.6	8.7
11	950	20	15	15	50	7.8	6.1	9.1	4.4
12	950	10	15	15	50	6.1	5.4	8.3	2.9
13	950	10	15	15	50	4.9	2.7	5.9	0.4
14	950	10	15	15	50	4.4	1.6	8.0	0.7
15	950	10	15	30	67	0.0	2.7	4.0	-0.1
16	950	10	15	15	50	0.0	3.3	7.1	0.7
17	950	20	10	10	50	4.4	2.1	6.1	0.8
18	950	10	120	240	33	0.9	1.2	3.4	-0.9
19	950	10	60	28.5	67	10.0	2.3	6.2	1.8
20	950	20	120	57.1	67	8.7	7.6	9.6	5.8
21	950	20	60	120	33	1.3	-0.7	0.5	-1.3
22	1,150	15	90	90	50	5.2	4.0	6.2	1.8
23	1,150	15	90	90	50	6.0	3.9	9.1	1.4
24	1,300	10	600	0	100	21.1	15.6	16.0	13.0
25	1,300	20	30	30	50	14.9	14.0	14.0	12.9
26	1,300	20	15	30	33	7.7	6.6	9.9	6.9
27	1,300	20	30	15	67	21.6	19.1	20.9	17.1
28	1,300	20	15	15	50	18.6	16.8	15.2	12.8
29	1,300	20	2	13	15	1.9	0.7	2.3	1.1
30	1,300	1	60	0	100	0.8	-0.1	1.4	-0.3
31	1,300	1	15	15	50	0.4	-0.2	0.8	-0.2
32	1,300	20	15	15	50	8.9	5.4	11.2	5.1
33	1,300	20	20	10	67	17.0	15.1	22.0	13.8
34	1,300	20	5	10	33	7.6	4.6	7.2	2.8
35	1,300	10	60	120	33	4.0	2.5	4.5	0.8
36	1,300	10	120	57.1	67	13.4	11.6	20.7	8.8
37	1,300	20	60	28.5	67	22.6	18.7	22.4	16.5
38	1,300	20	120	240	33	4.5	3.6	7.3	1.3

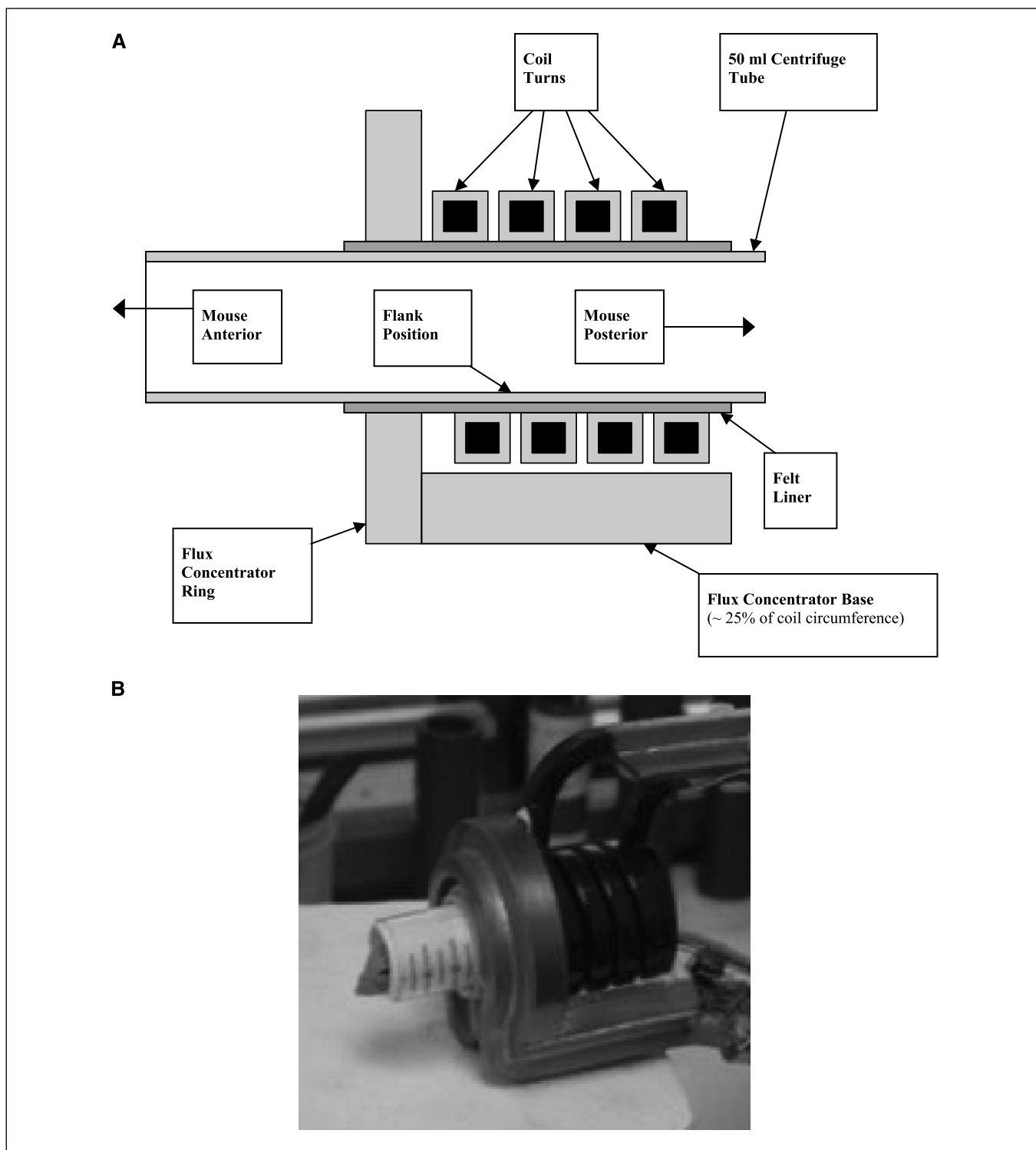


**Fig. 1.** Cross-sectional view of inductor displaying coil, flux concentrator ring and base, 50-mL conical tube, and felt lining in schematic (A). Photograph of mouse in inductor before exposure to AMF (B).

factors studied are not mutually independent, or orthogonal. Duty is an explicit ratio of ON and OFF times (Eq. B) and should therefore be separated during analysis. Conversely, duty is a measure of average power (or average “dose”), and for comparisons among specific ON/OFF combinations, it is natural to consider the effects of pulse width by choosing a combination of duty-ON time or duty-OFF time.

Therefore, two separate analyses of the data were done in addition to that using the combination of field amplitude, duration, and duty. Specifically, the combination of field amplitude, duration, ON time, and OFF time was analyzed to determine effects of pulse width on temperature, independent of duty. These results were compared against an analysis using the combination of field amplitude, duration, duty, and ON time.

**Results**

Table 1 contains a summary of AMF exposure conditions and final uncorrected rectal temperatures for the mice, whereas Table 2 provides a summary of  $\Delta T_{\text{corr}}$  for all temperature probes. Mice that experienced final rectal temperatures approaching or exceeding  $42^{\circ}\text{C}$  consistently died, with one exception, for which a rectal temperature of  $47.3^{\circ}\text{C}$  was recorded (data not shown). This datum was excluded from analysis by standard statistical criteria.

Mice exposed to field amplitudes in excess of 950 Oe and at duties  $>50\%$  experienced consistent morbidity and injury. In these mice, maximum uncorrected rectal temperature approached or exceeded  $42^{\circ}\text{C}$  (Table 1), and  $\Delta T_{\text{corr}}$  was observed to be greater than  $\sim 12^{\circ}\text{C}$  (Table 2). The average start temperature for all mice was  $30.5 \pm 0.3^{\circ}\text{C}$  for the rectum,  $29.0 \pm 0.2^{\circ}\text{C}$  for the skin,  $30.7 \pm 0.3^{\circ}\text{C}$  for the flank, and  $28.8 \pm 0.3^{\circ}\text{C}$  for the spine.

When injury or death occurred, necropsies of mice that died within 48 hours after AMF exposure (Table 1) showed consistent findings. The skin under the first inductor turn was noticeably red. Sometimes the exterior of the hind legs showed petechiae. Inside the abdomen, intestine that had been within the first inductor turn closest to the abdominal wall were red but not hemorrhagic. The cecum sometimes showed petechiae. Intestine deeper in the abdomen were pale and sometimes blanched. Lungs were red but not hemorrhagic. By comparison, necropsy results were normal in all respects of the one mouse randomly selected from the group showing no sign of injury (Table 1).

Observed temperature changes (i.e.,  $\Delta T$ ) with time as a response to AMF amplitude of 1,300 Oe and 33% duty for temperature probes placed on the skin and in the rectum are shown in Fig. 2A and B, respectively. These temperatures are not corrected against controls and represent ON/OFF combinations of 5/10, 15/30, and 120/240 seconds corresponding, respectively, to mouse numbers 34, 26, and 38 in Tables 1 and 2.

Fitting the model equation (Eq. C) to corrected temperatures ( $\Delta T_{\text{corr}}$ ) with field, duty, and duration as factors produced statistically significant ( $P < 0.05$ ) results for spine, flank, skin, and rectal temperature responses for cubic (total sum of exponents,  $\leq 3$ ) combinations of the factors and their interactions. Contributions from higher order terms (i.e., exponent  $> 3$ ) were not significant nor was a model that included these terms. Other statistical measures of significance such as  $R^2$  values, analysis of residuals and outliers, lack of fit tests, and tests of adequate precision (signal to noise) confirm the validity of the model. Thus, analysis and predictions within the variable space were validated.

The resulting model equation was used to generate a series of two-dimensional contour plots on which contour lines represent isotherms of response (constant  $\Delta T_{\text{corr}}$ ). A sample of contour plots for 20-minute exposure showing the relationship between duty and field amplitude for spine, flank, skin, and rectal temperature responses is displayed in Fig. 3. The contour plots show that the variable space displayed was well represented by experiment. Note, however, that the circles represent conditions at which data were taken and do not indicate the measured  $\Delta T_{\text{corr}}$  nor do they indicate by their placement a relationship with the predicted  $\Delta T_{\text{corr}}$ .

The effects of duration of exposure on rectal  $\Delta T_{\text{corr}}$  are compared in Fig. 4A to C for 5-, 10-, and 20-minute exposures at 400 Oe (Fig. 4A), 700 Oe (Fig. 4B), and 1,300 Oe (Fig. 4C). In general, increasing  $\Delta T_{\text{corr}}$  accompanies increasing duration of exposure and duty. However, at low duties and low-amplitude AMF (Fig. 4A-B), long durations in the coil do not produce substantial temperature increases and may even accompany a decrease of rectal  $\Delta T_{\text{corr}}$ . This indicates that AMF heating is insufficient to overcome heat loss. With AMF amplitudes of  $>700$  Oe, sufficient eddy current heating occurs at duties  $>50\%$ , eventually becoming acute and leading to adverse events. However, at the highest amplitudes ( $\sim 1,300$  Oe), duty has a profound effect on AMF-induced eddy current heating (cf. Fig. 4C).

A similar analysis was done for field amplitude, duration, ON time, and OFF time. These factors produced statistically

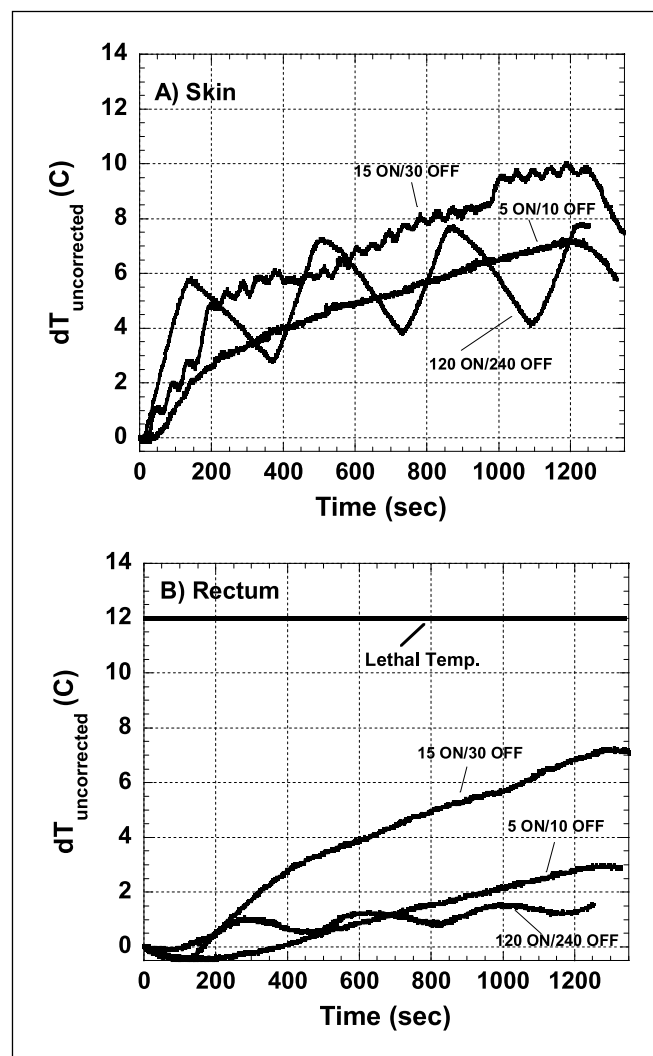
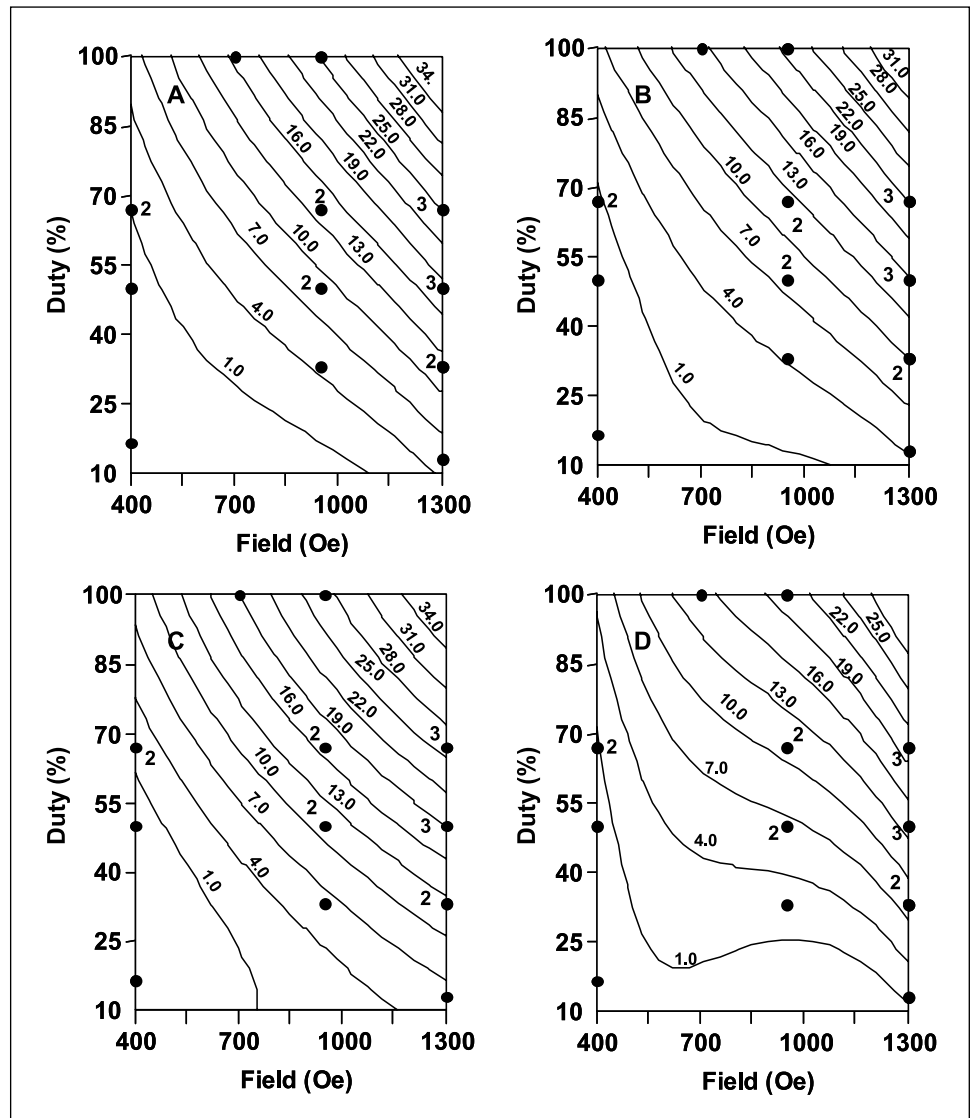


**Fig. 2.** Comparison of temperature response at fixed duty (33%) with varying pulse width obtained by probes placed on the skin of a hind limb (A) and inserted into the rectum (B). AMF conditions were 1,300 Oe and 33% duty. Total duration of exposure in each case was 20 minutes (1,200 seconds). Labels indicated pulse width with 5-second ON/10-second OFF, 15-second ON/30-second OFF, and 120-second ON/240-second OFF. Temperatures were recorded at 1-second intervals, and initial temperature at the start of AMF exposure ( $t = 0$  seconds) was subtracted from subsequent temperatures. Solid line at  $\Delta T = 12^{\circ}\text{C}$  indicates the observed temperature threshold associated with adverse events.

**Fig. 3.** Contour plots showing  $\Delta T_{\text{corr}}$  isotherms for spine (top left), flank (top right), skin (bottom left), and rectum (bottom right) as a function of duty (%) and field amplitude (Oe) for a 20-minute exposure. Contour lines were generated from the results of fitting an empirical model (see text) to temperature data observed for varying field amplitude, duty, and duration of exposure. Solid circles denote AMF conditions for which temperature data were taken and do not indicate measured  $\Delta T_{\text{corr}}$  values. Integers associated with a solid circle indicate the number of trials, when  $>1$ , conducted at the AMF conditions specified by the location on the plot of the circle.



significant ( $P < 0.05$ )  $\Delta T_{\text{corr}}$  responses for only linear combinations of the factors and their interactions. Unlike the previous analysis, not all factors were significant in the statistical analysis. Only field, field-duration, and duration-OFF time combinations were statistically significant factors in the response. Other statistical measures confirmed the validity of the model; however, by comparison with the first model, the SEs of the estimated coefficients were larger. This perhaps indicates that a greater number of data points are required due to the additional factor. Still, the model provides an adequate signal and is valid for predicting  $\Delta T_{\text{corr}}$  within the design space.

In a final analysis the effects of field amplitude, duration, duty, and ON time on  $\Delta T_{\text{corr}}$  were compared. Statistical measures of validity were similar to those obtained for the field-duration-ON-OFF analysis and even slightly better. Both models produced qualitatively similar predictions for  $\Delta T_{\text{corr}}$  when analogous combinations of the respective factors were used.

Because four factors were used to analyze the effect of pulse width (i.e., field, duration, and OFF and ON times), the resulting response surface occupies a four-dimensional volume.

This situation also exists for the combination of field-duration-duty-ON time. Because the combination of field-duration-duty-ON time provides a natural comparison of the effects of pulse width on rectal  $\Delta T_{\text{corr}}$  at constant power and because a rigorous comparison of the two analyses produced substantially similar results, the results of modeling the combination of field-duration-duty-ON time are presented. Figure 5 shows a representative series of contour plots generated from the model equation showing rectal  $\Delta T_{\text{corr}}$  for various combinations of duration and duty at 950 Oe with varying ON times (Fig. 5A-C). Shading, a measure of the SE, within the plots indicates a relatively high degree of uncertainty, with  $\pm 3^\circ\text{C}$  for darkest shading. Thus, quantitative predictions obtained from the model are limited.

Nevertheless, the trend of decreasing rectal  $\Delta T_{\text{corr}}$  with increasing ON (and therefore OFF) at constant duty is apparent. Particularly interesting is the change of rectal  $\Delta T_{\text{corr}}$  isotherms, which are generally increasing with increasing duration at constant duty and ON times of 15 and 60 seconds (Fig. 5A and B, respectively), and then tend to remain constant for increasing duration at a given duty (Fig. 5C).

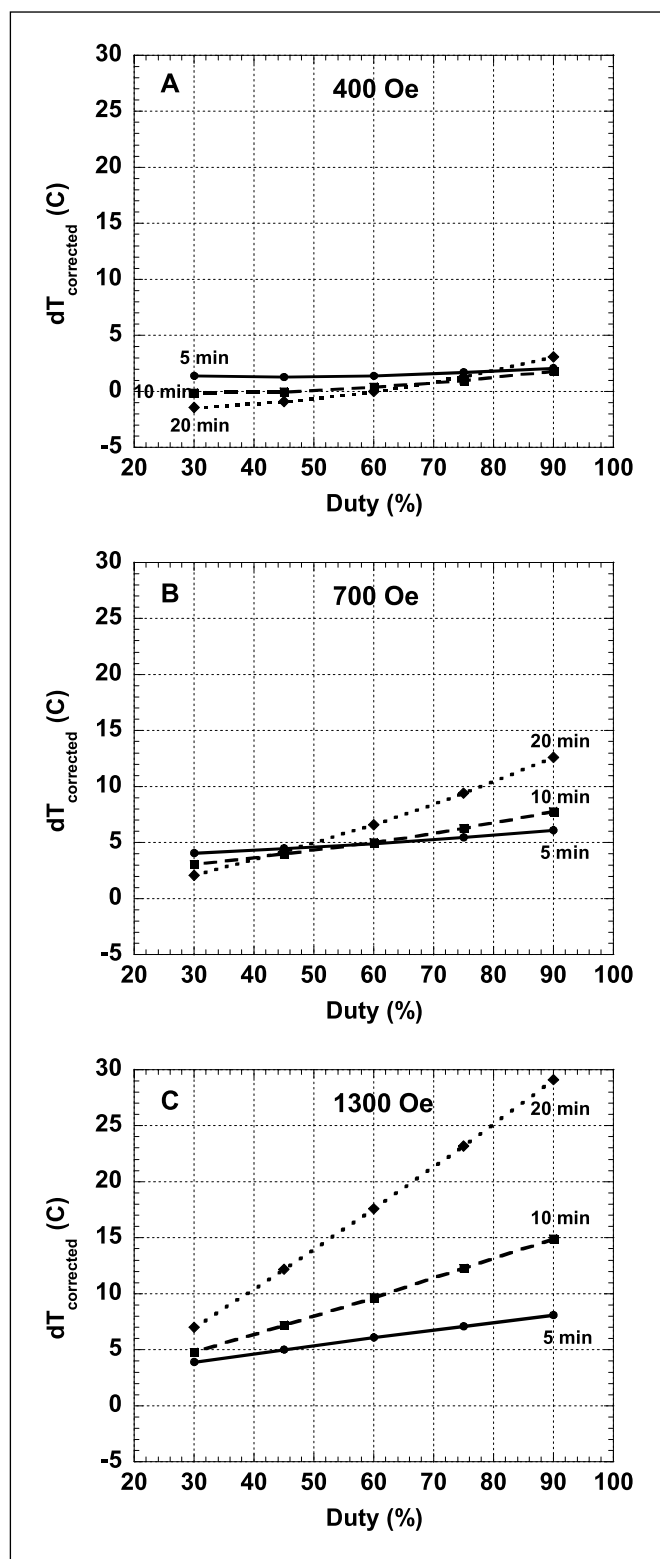


Fig. 4. Predicted rectal  $\Delta T_{corr}$  values obtained for 5-, 10-, and 20-minute duration of exposure to AMF with duty, as shown in Fig. 2D. Field amplitudes are 400 Oe (A), 700 Oe (B), and 1,300 Oe (C).

The trend of increasingly effective tissue temperature regulation for increased ON/OFF time for specific amplitude and duty combinations is further illustrated in Fig. 6A to C

where duty is constant at 50%. At low fields (400 Oe; Fig. 6A), there is insufficient power deposition to create a net increase of rectal  $\Delta T_{corr}$ , regardless of ON time and duration of exposure. Indeed, a net loss of heat occurs with increased duration of exposure and ON time, as seen in Fig. 4. However, at 950 Oe (Fig. 6B), the combination of short ON time (5 seconds) and long duration (20 minutes) deposits a sufficient eddy current heating to approach a toxic threshold of  $\Delta T_{corr} = 13^\circ\text{C}$ . However, further increasing the ON time to 90 seconds results in an apparently more effective *in vivo* temperature regulation yielding a net increase of  $\Delta T_{corr} \approx 3^\circ\text{C}$  that remains unchanged even at a 20-minute exposure, suggesting an equilibrium of heat input and output has been established. For 1,300 Oe (Fig. 6C), this equilibrium occurs at  $\Delta T_{corr} \approx 5^\circ\text{C}$  and 180 seconds ON time. On the other hand, a 5-second ON time produces a net increase of rectal  $\Delta T_{corr}$  with increasing duration of exposure, such that at 20 minutes, the toxic threshold will probably be exceeded.

### Discussion

AMF can be used to heat magnetic nanoparticles localized in tissue (e.g., cancer) by specific antibodies. To effectively heat the cancer, it is advantageous to subject the particles to high-amplitude AMF of sufficient duration. This unique treatment approach takes advantage of the particle SAR, measured in W/g material, to focus heat on the cancer cells to initiate thermoablative therapy. Provided the AMF can be applied in a manner that limits net tissue temperature increase, healthy tissues are not subjected to extreme heat and are spared.

One way to reduce eddy current heating is to limit the area of exposure to high-amplitude fields. An induction coil was designed and manufactured to take advantage of mouse geometry and confine the area of high-amplitude AMF to a 1-cm-wide region inside the coil. The field distribution within the coil was inhomogeneous, thereby minimizing exposure to high-amplitude AMF in unintended areas. Placing magnetic flux controlling material on the coil achieved further reductions of flux in these areas.

No adverse events occurred for mice exposed to continuous AMF (100% duty) for amplitudes of 700 Oe and all durations (Table 1). Adverse events occurred for mice exposed for 20 minutes to continuous AMF at 100% duty and amplitudes of >700 Oe, with rectal temperatures approaching or exceeding  $42^\circ\text{C}$ . Whereas the sample size of this study was insufficient to determine the precise threshold for adverse events associated with AMF exposure, our observations are consistent with those made by others that core temperatures  $\geq 42^\circ\text{C}$  are potentially lethal (13).

More information was obtained from the data by fitting an empirical model to the  $\Delta T_{corr}$  data when field, duration, and duty were explicitly modeled. Assuming that a  $\Delta T_{corr} = 13^\circ\text{C}$  is lethal, then a 20-minute exposure to field amplitudes as low as ~630 Oe and 100% duty can be lethal (cf. Fig. 3). This value is consistent but lower than might be predicted from inspection of Table 1.

Pulsing the AMF reduces heating by reducing total power deposited due to eddy current production and providing opportunity for heat dissipation during the OFF time. A linear relationship between  $\Delta T_{corr}$  and duty for a given field

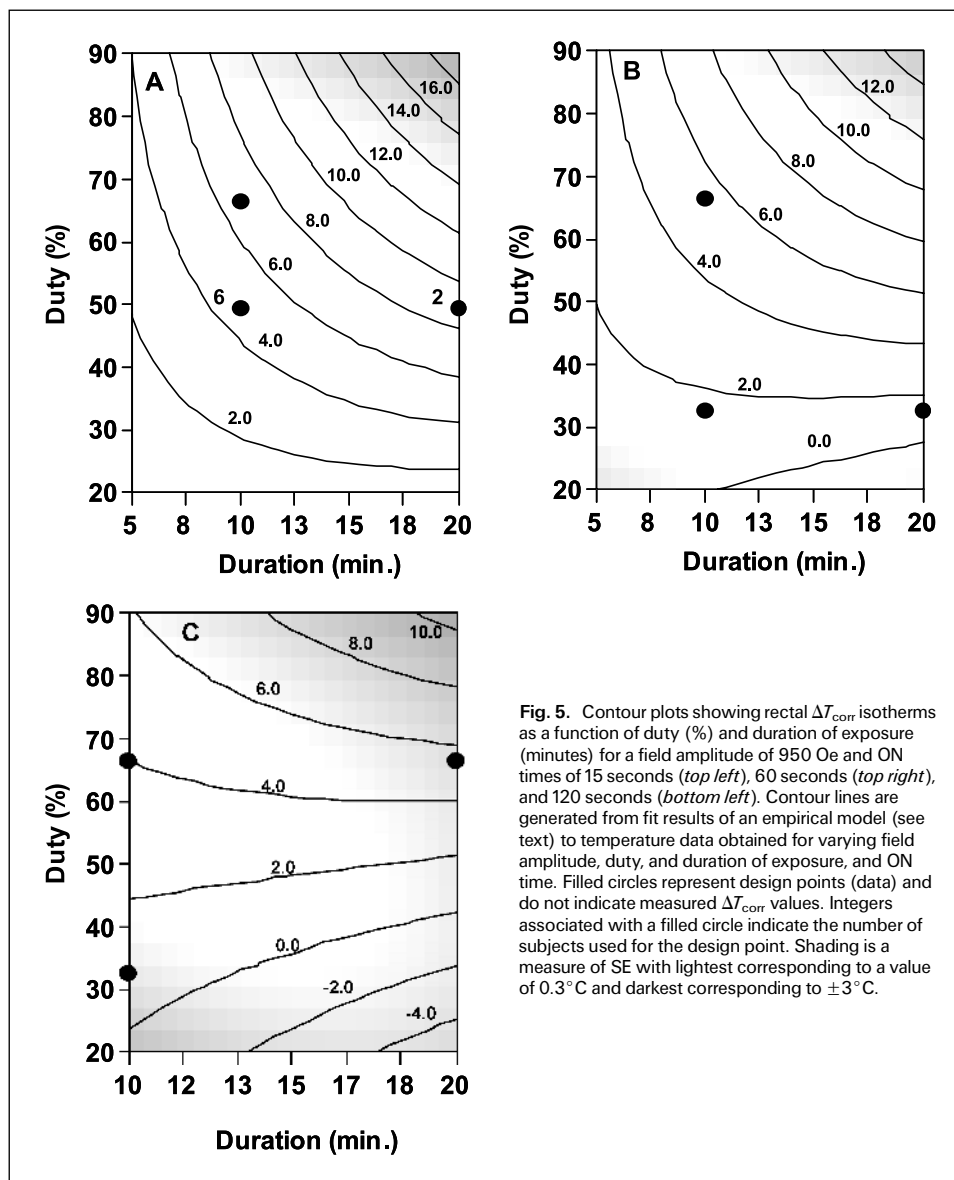


Fig. 5. Contour plots showing rectal  $\Delta T_{\text{corr}}$  isotherms as a function of duty (%) and duration of exposure (minutes) for a field amplitude of 950 Oe and ON times of 15 seconds (top left), 60 seconds (top right), and 120 seconds (bottom left). Contour lines are generated from fit results of an empirical model (see text) to temperature data obtained for varying field amplitude, duty, and duration of exposure, and ON time. Filled circles represent design points (data) and do not indicate measured  $\Delta T_{\text{corr}}$  values. Integers associated with a filled circle indicate the number of subjects used for the design point. Shading is a measure of SE with lightest corresponding to a value of  $0.3^\circ\text{C}$  and darkest corresponding to  $\pm 3^\circ\text{C}$ .

amplitude and duration is expected, because total power deposition due to eddy current production varies linearly with duty. Contour plots of field and duty at 20-minute duration (Fig. 3A-D) show that  $\Delta T_{\text{corr}}$  for spine, flank, skin, and rectum increases as duty is increased for a given field amplitude. The distance between successive  $\Delta T_{\text{corr}}$  isotherms seems constant for constant field, except at the lowest amplitudes and duties where some deviation from linearity appears. This apparent deviation is not significant, because in these regions the uncertainties are  $\pm 1^\circ\text{C}$ , comparable with the predicted  $\Delta T_{\text{corr}}$ .

The value of  $\Delta T_{\text{corr}}$  for the rectum is lower than the corresponding temperatures for the spine, flank, and skin, particularly at high amplitude and duty (cf. Fig. 3A-D and Table 2). In general, eddy current production is greatest in areas with large radius and zero at the electrical center (i.e.,  $r = 0$ ; cf. Eq. A). The temperature probe placed on the skin is at maximum  $r$  for the mouse, whereas the temperature probe placed in the rectum is near the electrical center (i.e.,  $r \approx 0$ ). The temperature probe placed on the skin provides a direct

measure of eddy current heating during an ON cycle, with concomitant heat loss during an OFF cycle (Fig. 2A). Hence, temperature oscillations due to pulsing are pronounced, particularly with long ON/OFF cycles.

On the other hand, the temperature probe placed in the rectum does not measure eddy current heating directly but rather the net heat balance resulting from heating of the surrounding tissue during exposure to AMF, thermoregulatory response to eddy currents, heat loss to the environment (coil), and heat produced by metabolic processes. Consequently, temperature oscillations seem damped (Fig. 2B) when compared against skin measurements (Fig. 2A). Because mortality is associated more directly with core temperature (i.e., rectal; refs. 12, 13), maintaining a rectal temperature within safe limits has significant implications for the safe application of AMF.

Eddy current heating is most affected by duty at the highest amplitudes ( $\sim 1,300$  Oe; Fig. 4). That duty has such an effect upon  $\Delta T_{\text{corr}}$  for AMF exposure is not surprising as this is directly related to average power or dose, even for mice, which are

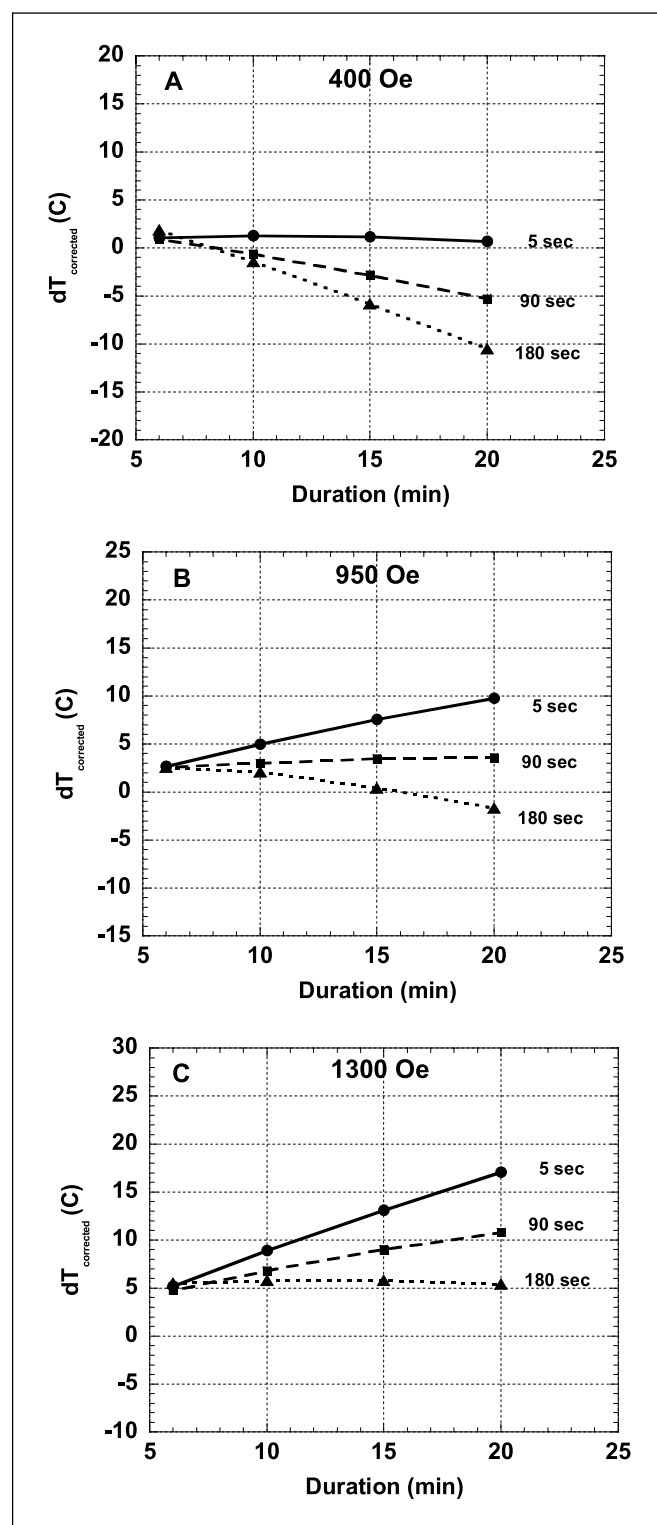


Fig. 6. Predicted rectal  $\Delta T_{\text{corr}}$  values obtained for 5-, 90-, and 180-second ON times with duration of exposure at 50%. Field amplitudes are 400 Oe (A), 950 Oe (B), and 1,300 Oe (C).

known to have poor thermoregulatory systems (12), compared with humans. In addition to decreasing the total eddy current heating in the mouse, decreasing duty also provides time for heat dissipation during OFF cycles.

The effect of ON/OFF pulse variation for a given duty and amplitude was observed directly as illustrated in temperature plots shown in Fig. 2. Increasing ON time from 5 to 15 seconds results in an increase of eddy current heating and a net increase in temperature. However, this trend is reversed for very long ON/OFF cycles ( $\geq 15$  seconds ON and  $\geq 30$  seconds OFF), provided one ON cycle does not produce an acute level of eddy current heating (cf. Tables 1 and 2). Within this constraint, very long ON/OFF cycles can produce a net rectal temperature (Fig. 2B) that is substantially lower than that produced by short ON/OFF AMF exposure even after a 20-minute duration (Figs. 4 and 5). This is an intriguing observation.

Analysis of the data taking into account pulse width provides further evidence of the complex interaction of AMF power deposition (or tissue SAR) through eddy current production and resulting changes in tissue temperature. Contour plots showing rectal  $\Delta T_{\text{corr}}$  isotherms as a function of duty and duration of exposure for 950 Oe that result from an analysis of temperature response to the factors field amplitude-duration-duty-ON time is shown in Fig. 5A to C, where ON time is varied from 15 seconds (Fig. 5A) to 120 seconds (Fig. 5B). As ON time increases, the temperature in the rectum decreases, particularly at high duty and long duration of exposure, as does the slope and curvature of the individual isotherms. This qualitative change in temperature response with ON time suggests a profound shift in thermoregulatory response to AMF eddy current production as ON time is increased when field amplitude and duty, or total AMF "dose", are held constant.

This effect is further illustrated in Fig. 6A to C, which show a comparison of predicted rectal  $\Delta T_{\text{corr}}$  for a duty of 50% and ON times of 5, 90, and 180 seconds for field amplitudes of 400 Oe (Fig. 6A), 950 Oe (Fig. 6B), and 1,300 Oe (Fig. 6C). Note that for each field amplitude the average AMF "dose" (or tissue SAR) is constant, because it is defined by field amplitude, frequency, radius of exposure (cf. Eq. A), and duty. Conversely, the physiologic temperature response to this dose is complex and can vary dramatically depending upon the algorithm used to apply the AMF *in vivo*. Such a complex relationship of power deposition, tissue SAR, and tissue temperature response has been reported in both preclinical and clinical trials using microwave antenna arrays (12, 14–18) and ultrasound (19) for the treatment of cancer. Although the clinical significance of these observations at the frequency chosen in this study is unknown, it provides an interesting line for further investigation.

Safe application of high-amplitude AMF sufficient to heat antibody-conjugated magnetic nanoparticles (bioprobes) localized in cancer tissue is possible provided the area of exposure and duty are controlled. The choice of duration and duty at amplitudes  $>700$  Oe are integral to limit nonspecific heating. Results presented suggest that pulse width is also important for safety and can be maximized, within limits, to apply a high thermal dose locally with nanoparticles to cancer cells. Under such conditions, heat delivered by bioprobes can potentially be modulated by suitable selection of AMF variables to enhance a therapeutic effect, whereas normal tissues can recover and dissipate heat produced by eddy currents during OFF times.

### Acknowledgments

We thank Dr. Douglas Gwost and Carmen Traxler for their contributions to the study design and Laird Meiers for mouse care and handling.

## References

1. Overgaard J. History and heritage: an introduction. In: Overgaard J, editor. *Hyperthermic oncology*. Vol. 2. London: Taylor and Francis; 1985. p. 8–9.
2. Streffer C, van Beuningen D. The biological basis for tumor therapy by hyperthermia and radiation. In: Streffer J, editor. *Hyperthermia and the therapy of malignant tumors*. Berlin: Springer; 1987. p. 24–70.
3. Zaffaroni N, Fliorentini G, De Giorgi U. Hyperthermia and hypoxia: new developments in anticancer chemotherapy. *Eur J Surg Oncol* 2001;27:340–2.
4. Hildebrandt B, Wust P, Ahlers O, et al. The cellular and molecular basis of hyperthermia. *Crit Rev Oncol Hematol* 2002;43:33–56.
5. Moroz P, Jones SK, Gray BN. Tumor response to arterial embolization hyperthermia and direct injection hyperthermia in a rabbit liver tumor model. *J Surg Oncol* 2002;80:149–56.
6. Moroz P, Jones SK, Gray BN. Magnetically mediated hyperthermia: current status and future directions. *Int J Hyperthermia* 2002;18:267–84.
7. Jeffrey S, Birdwell R, Ikeda D, et al. Radiofrequency ablation of breast cancer: first report of an emerging technology. *Arch Surg* 1999;134:1064–2008.
8. Izzo F, Barnett CC, Curley SA. Radiofrequency ablation of primary and metastatic malignant liver tumors. *Adv Surg* 2001;35:225–50.
9. Gordon RT, Hines JR, Gordon D. Intracellular hyperthermia: a biophysical approach to cancer treatment via intracellular temperature and biophysical alteration. *Med Hypotheses* 1979;5:83–102.
10. Jordan A, Wust P, Scholz R, Faehling H, Krause J, Felix R. Magnetic fluid hyperthermia (MFH). In: Hafeli U, et al, editors. *Scientific and Clinical Appl Magn Carriers*. New York: Plenum Press; 1997. p. 569–95.
11. Jordan A, Scholz R, Wust P, Fahling H, Felix R. Magnetic fluid hyperthermia: cancer treatment with AC magnetic field induced excitation of biocompatible superparamagnetic nanoparticles. *J Mag Mat* 1999;201:413–9.
12. Adair ER, Black DR. Thermoregulatory responses to RF energy absorption. *Bioelectromagnetics* 2003;6:S17–38.
13. Dewhirst MW, Viglianti BL, Lora-Michiels M, Hanson M, Hoopes PJ. Basic principles of thermal dosimetry and thermal thresholds for tissue damage from hyperthermia. *Int J Hyperthermia* 2003;19:267–94.
14. Mechling JA, Strohbehn JW, Ryan TP. Three-dimensional theoretical temperature distributions produced by 915 MHz dipole antenna arrays with varying insertion depths in muscle tissue. *Int J Radiat Oncol Biol Phys* 1992;22:131–8.
15. Ryan TP. Comparison of six microwave antennas for hyperthermia treatment of cancer: Sar results for single antennas and arrays. *Int J Radiat Oncol Biol Phys* 1991;21:403–13.
16. Ryan TP, Mechling JA, Strohbehn JW. Absorbed power deposition for various insertion depths for 915 MHz interstitial dipole antenna arrays: experiment versus theory. *Int J Radiat Oncol Biol Phys* 1990;19:377–87.
17. Tremblay BS, Douple EB, Ryan TP, Hoopes PJ. Effect of phase modulation on the temperature distribution of a microwave hyperthermia antenna array *in vivo*. *Int J Hyperthermia* 1994;10:691–705.
18. Ryan TP, Hoopes PJ, Taylor JH, et al. Experimental brain hyperthermia: techniques for heat delivery and thermometry. *Int J Radiat Oncol Biol Phys* 1991;20:739–50.
19. Ryan TP, Hartrov A, Colacchio TA, Coughlin CT, Stafford JH, Hoopes PJ. Analysis and testing of a concentric ring applicator for ultrasound hyperthermia with clinical results. *Int J Hyperthermia* 1991;7:587–603.